

# Computer simulation studies of low-temperature hopping in spatially and energetically disordered systems

J. M. MARSHALL

Professor Emeritus, School of Engineering, University of Wales Swansea, U.K.

(Address for correspondence: 64 Ridgeway, Killay, Swansea SA2 7AP, U.K.)

Quantum mechanical tunnelling between localised sites can dominate carrier transport in sufficiently disordered solids. We examine such transport, employing a Monte Carlo simulation technique. Initially, the advantages and drawbacks of this approach are indicated. The discrepancies between the mobility and the diffusion coefficient under transient thermalisation conditions are then examined. Attention is next turned to the low-temperature "variable range" hopping regime. The conceptual error in the derivation of the "Mott  $T^{-1/4}$ " law is reviewed, and a new approach is then advanced. This is shown to be in very good agreement with the simulation data, in respect of the dominant hopping distance and the density of states close to the Fermi level. Finally, we question whether *any* such model can be expected to yield meaningful results, when applied to experimental data.

(Received November 1, 2006; accepted December 21, 2006)

**Keywords:** Disordered semiconductors, Variable range hopping, Mobility, Diffusion

## 1. Introduction

Positional and energetic disorder generates localised defect states within the energy gap of an otherwise perfectly ordered material. When the concentration of such states is sufficiently high and/or the temperature is sufficiently low, carrier transport by quantum mechanical tunnelling ("hopping") can replace transport in extended states as the dominant mechanism [1].

Most prior examinations of this situation have utilised analytical techniques involving various important assumptions and simplifications. In particular, despite a fundamental error in its formulation (see below), the "Mott  $T^{-1/4}$  variable-range hopping" model [1] continues to be applied to estimate (e.g.) the density of states close to the Fermi level,  $N(E_f)$ , from experimental data. There is also a problem concerning the validity or otherwise of the Einstein relationship between the carrier mobility and diffusion coefficient during the relaxation of excess charge carriers towards quasi-thermal equilibrium. To address these problems, we constructed a large computer-generated random array of sites, and examined hopping transport within it, using a Monte Carlo technique.

After outlining the technique, the paper proceeds by addressing the problem of the "anomalous" relationship between the drift mobility and diffusion coefficient, during the thermalisation of excess charge carriers.

It continues by examining the temperature dependence of these parameters under quasi-thermal equilibrium conditions at low temperatures. The resulting data are then considered in terms of the Mott  $T^{-1/4}$

model, and of a new alternative analytical technique that is shown to provide more satisfactory agreement.

Finally, the likelihood that *any* such model of low-temperature hopping can yield reliable data in respect of parameters such as  $N(E_f)$  is assessed.

## 2. The Monte Carlo simulation procedure

The rate of carrier jumps from a site of energy  $E$  to one at  $E'$ , over a distance  $r$ , is normally described via the Miller-Abrahams [2] expression:

$$v_j = v_0 \exp\left(-\frac{2r}{r_0}\right) \left\{ \begin{array}{l} \exp\left[-\frac{E-E'}{kT}\right], (E > E') \\ 1 \quad (E < E') \end{array} \right\} \quad (1)$$

Here,  $v_0$  is the "attempt to hop" frequency ( $10^{12}$  Hz throughout this study),  $r_0$  is the localisation length for the sites (0.4 simulation units throughout (relative to a mean site density of 1 simulation unit - see Fig. 1)), and  $T$  the temperature. At finite applied fields,  $E-E'$  is modified by the additional field-induced potential difference between the two sites. In this study, the applied field was chosen to give values much less than  $kT$  between nearest (and allowed higher-order) neighbour sites, to avoid field-induced effects upon the carrier mobility and diffusion. It was also set to zero in some cases, to allow the study of diffusion alone.

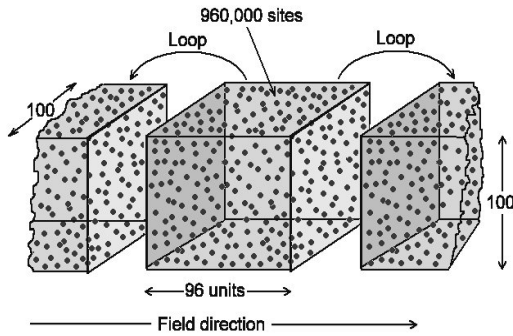


Fig. 1. The localised site array used in the Monte Carlo simulations.

As illustrated in Fig. 1, the array employed in these studies comprised 960,000 hopping sites, randomly distributed in a volume of  $96 \times 100 \times 100$  units, and randomly assigned energies between 0 and  $0.2eV$  above the Fermi level,  $E_f$ , (set at  $0.6 eV$  here). For each site, the identities of the 8 (or later 16) nearest neighbours (i.e. those with the highest values of  $v_j$ ) were determined, for each temperature and field. The first and last regions close to  $x = 0$  and  $x = 96$  were linked using periodic boundary conditions, allowing carriers to cross the boundaries and thus providing *notionally* infinite allowed diffusion and drift distances. (Note - this requires a sufficiently large array to fully represent the "bulk" material, including all important variations in the local environment. With a total of 960,000 sites, we believe that this assumption is justified in the present case).

Note that the term "Fermi level" is used very loosely above and elsewhere in this paper, since we have not (so far) included finite-temperature Fermi-Dirac occupation statistics. Thus all states above  $E_f$  are taken as empty, and all those below it as full (or non-existent in the present case). Of course, this simplification also applies in respect of the Mott  $T^{-1/4}$  model, with which we compare our present simulation results. The effects of including the full finite temperature statistics are being investigated in our further studies.

The Monte Carlo simulation of hopping within this array featured the usual steps, as outlined in [3], for example.

## 2.1. Advantages and limitations of the Monte Carlo approach

The most attractive feature of the Monte Carlo approach is that it can reduce any underlying assumptions, or the effects of averaging procedures (as employed in alternative approaches such as those proposed in [4]) to a minimum. It can also thereby provide valuable insights into the distortions that such simplifications may generate.

A counterbalancing disadvantage, in the case of hopping transport, is that it requires extremely long computation times. A carrier that chances upon two

extremely closely adjacent sites can hop backwards and forwards between them very many times before it moves on. The actual hopping times for such transitions will normally be very short in comparison to the rate-limiting ones, so such events are not expected to determine the longer-time behaviour. However, the *computation time* required for each such hop is the same as for any others over greater distances, and thus controls the overall timescale of the simulation!



Fig. 2. Schematic illustration of a complex multi-site trapping configuration.

Moreover, in the present case of hopping at low temperatures, the effect is not confined to such "intimate pairs" of neighbour sites. For example, Fig. 2 depicts an interconnected set of sites, detected by inspection within the present array at  $T = 6 K$ . The eight nearest neighbours of site 0 are shown, with site 1 being the very nearest neighbour and so forth. Note that:

(i) Most of the sites numbered 1-8 also have neighbours within the set (only the 1st to 4th neighbours are shown, to avoid clutter, but inclusion of the higher order (5-8) neighbour links yields an even greater internal connectivity).

(ii) The fractional probability of returning directly from site 1 to site 0 is 99.8%, as is the probability of returning from site 2 to either site 0 or site 1.

(iii) Even carriers that escape these three sites have a very high probability of returning to them. This is also the case for carriers that eventually manage to escape the cluster as a whole.

(iv) Thus, there are relatively few avenues of escape from the cluster, although the carrier will eventually do so.

The above situation raises the question of whether allowing carrier transitions to only the 8 nearest neighbours of an occupied site is sufficient. For example, in the extreme case in which the restriction was to allow transitions to only the 1st and 2nd nearest neighbours, sets of three sites which are all the 1st or 2nd neighbours of each other would occur. These would then constitute "black holes", from which a carrier could never escape [4]. Of course, this probability decreases as the number of allowed neighbours increases, and the configuration in Fig. 2 does not strictly constitute a "black hole" (i.e. there are low-probability avenues of eventual escape). Even so, the restriction of transitions to 8 neighbours is questionable, particularly at very low temperatures. Thus, the number of allowed neighbours was increased to 16 in some circumstances below.

### 3. Time-dependent carrier mobility and diffusion, under transient conditions

One objective of the present investigation was to examine the relaxation of excess charge carriers toward their ultimate steady-state (Maxwell-Boltzmann) energy distribution. The Monte-Carlo procedure can provide data on the time dependence of the mean carrier displacement,  $\bar{x}$ , under an applied field, plus the actual carrier spatial distribution and the RMS deviation from the mean position. It can also provide the energy distribution as a function of time, as will be illustrated below.

In this primary study, to provide a significant difference between the initial and final energy distribution, each carrier was initially selected at random within the array, thus giving it a random energy within the range 0.4 to  $E_f (= 0.6)$  eV. Obviously, this also generated a random starting position, so that all subsequent displacements were calculated relative to this. Data for a sufficiently large number of carriers were then compiled, to give the behaviour of the overall carrier ensemble.

It immediately became clear that the resulting values of the mobility, defined as

$$\mu' = d\bar{x}/dt, \quad (2)$$

did not agree in all circumstances with those calculated by applying the Einstein relation to the diffusion coefficient,  $D$ , as normally defined:

$$\mu_D = eD/kT, \quad (3a)$$

$$\sigma(t) = \sqrt{2Dt}, \quad (3b)$$

where  $\sigma(t)$  is the RMS dispersion of the carrier packet.

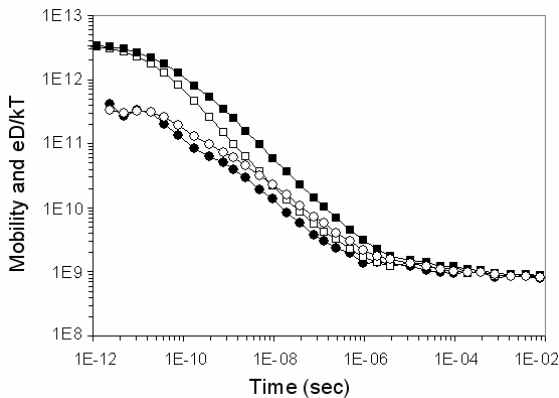


Fig. 3. Time dependence of the drift mobility and diffusion coefficient, as calculated from Eqs. 2 (filled circles), 3a (filled squares), plus Eqs. 4 (open squares) and 5 (open circles), as presented below ( $T = 20$  K and  $F = 5e-5$  in all cases).

Fig. 3 provides an illustration of this for the case  $T = 20$ K, and field  $F = 5e-5$  simulation units. Note that:

- (i)  $F$  was restricted to such a very low value to avoid distortion in the calculation of  $D$  due to the disproportionate influence upon the conventional RMS-based calculation, for those carriers which happen to be left well behind the main drifting carrier packet, due to atypically deep trapping;
- (ii) The mobility values are in simulation units - i.e. not multiplied by any more physically-realistic value of the actual mean inter-site separation, and
- (iii) The  $\mu'$  curve shows more noise than the  $\mu_D$  one, because of the very low field employed, and also because the former is calculated from a *time derivative* of the mean displacement.

The most obvious feature of Fig. 3 is the large discrepancy between the two calculated mobilities at short times (although they clearly converge at sufficiently long times). There are (at least) two contributory factors here. The first is that the drift mobility defined in Eq. 2 is an "instantaneous" value, as is the time-dependent current obtained in experimental studies. However, the diffusion coefficient defined in Eq. 3a incorporates *all prior diffusion* back to the initial carrier generation time. To address this problem, we have proposed [3] a revised definition of a (*time-dependent*) differential diffusion coefficient as:

$$D'(t) = (d\sigma^2/dt)/2, \quad (4)$$

with the resulting mobility,  $\mu'_D$ , then being calculated as in Eq. 3a.

For consistency, and for illustration of the conceptual difference, we have also calculated what the drift mobility would be, if simply calculated in terms of the mean position at time  $t$ :

$$\mu = \bar{x}/t. \quad (5)$$

Fig. 3 also shows the effects of employing the revised definitions,  $\mu$  and  $\mu'_D$ . It is immediately clear that (at least for this set of simulation parameters) the alternative definitions once more yield differences during the thermalisation regime (but again all converge when equilibration is approaching completion). However, although these distinctions of definition are obviously important in their own rights, they equally obviously fail to completely resolve the underlying disagreement between the various  $\mu$  and  $eD/kT$  values.

This can be (at least partly) explained by the fact that during the equilibration period, the carrier distribution profile is not, in general, Gaussian (as is implicitly assumed in the calculation of  $D$  via the RMS value in Eq. 3b).

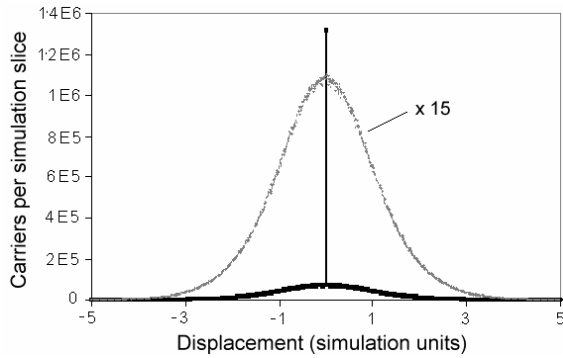


Fig. 4. Carrier distribution at  $1e-9$  sec ( $T = 20K$ ,  $F = 5e-5$ ). The heavy line is the computed distribution, and the lighter data points are an amplified version, without the central spike.

Fig. 4 illustrates such a situation during equilibration at 20K. About 9% of the carriers have remained in their initial locations, even at this intermediate stage. Note also that:

(i) At this point, the mean displacement due to the field is less than  $4e-3$  simulation units (hence the comparatively high noise levels in the mobility calculations), and

(ii) Aside from the central spike, the distribution is almost Gaussian. However, at some stages during the equilibration, we have observed more noticeable deviations (e.g., a Lorentzian distribution can sometimes provide a better fit).

A second factor is that during the equilibration period, the calculated mobility and diffusion values depend significantly upon the initial conditions.

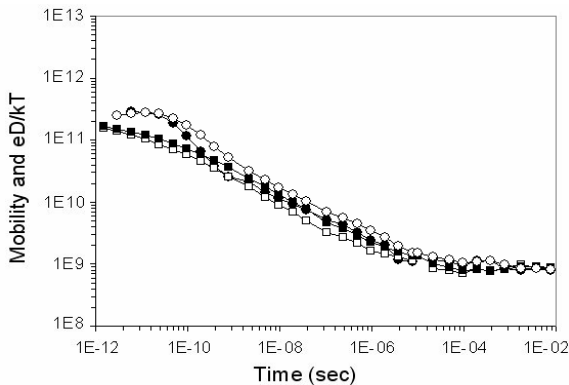


Fig. 5. Time dependence of the drift mobility and diffusion coefficient, as in Fig. 3, but with carriers launched only from sites within the bottom  $2kT$  of the energy distribution ( $T = 20 K$ ,  $F = 5e-5$ ).

As an example, Fig. 5 shows the situation in which all carriers were initially created only in those sites having energies within the bottom  $2kT$  of the distribution (as opposed to the free selection of energy employed previously). In this case, the relaxation is primarily dominated by equilibration within the spatial configuration of deep states.

Although the drift-derived mobilities are not greatly affected relative to those in Fig. 3, those calculated from the diffusion data are reduced by more than an order of magnitude at the shortest times. This is to be expected, since the initial carrier energy distribution is much closer to the final one. The reason why the drift values are much less affected is that in Eq. 1, the field only influences the probability of hops to shallower states, and most hops are initially downward in the case of Fig. 3. If the carriers were all launched within the very shallowest sites, their initial relaxation would be almost totally dominated by transitions to deeper sites, and the ratio of the diffusion-based to the drift-based mobilities would be even higher at short times. Thus, Fig. 3 represents an intermediate case, but one still dominated by relaxation in energy at short times.

Regrettably, given the complex nature of the situation, it does not appear realistic to attempt a more quantitative explanation of the relationships between the data in Figs. 3 and 5, or their equivalents at other temperatures etc.

Finally, in this Section, we note that the simulation technique can provide other useful information concerning the carrier relaxation process. As an example, Fig. 6 displays the evolution with time of the carrier energy distribution (simulation conditions as in Fig. 3).

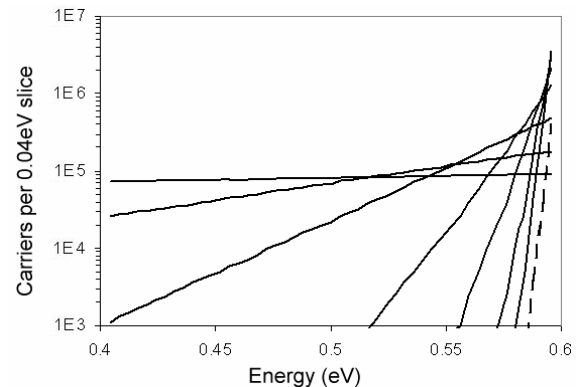


Fig. 6. Carrier energy distribution (conditions as in Fig.3), from  $10^{-12}$  to  $10^{-6}$  sec (in decade steps). The dotted line is the theoretical final distribution, to which the longer-time data converge.

#### 4. Low-temperature "variable range" hopping - The "Mott $T^{-1/4}$ " model

A second objective of this study was to explore the validity or otherwise of the low-temperature "variable-range" hopping concept. In particular, although many more elaborate analyses of this phenomenon (see e.g. [1] for references to these) have been advanced, our strong impression is that the only one (because of its attractive simplicity) which continues to be employed for quantitative calculations of the density of states close to  $E_f$  is that original formulated by Mott [5, 6].

Sadly, this contained a fundamental error! This was subsequently accepted by the model's originator, but is still not universally recognised. Thus, before proceeding, it remains appropriate to review the problem.

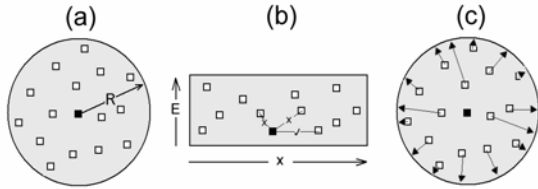


Fig. 7. Concepts involved in the Mott model for low temperature variable range hopping.

Consider sites that are uniformly distributed in energy close to  $E_f$ , with a concentration  $N(E_f)$ . A sphere of radius  $r$  (Fig. 7a) will on average contain  $4\pi r^3 N(E_f)/3$  sites, giving an average energy separation of  $W = 3/(4\pi r^3 N(E_f))$ . This will obviously decrease as  $r$  increases. (Note that, as in the present simulations, this formalism implies the use of zero-temperature occupation statistics, in that all of these sites are assumed to be empty).

The model proceeds by using this value of  $W$  in conjunction with Eq. (1) and conventional diffusion theory, to give:

$$\mu_{\text{hop}} = (e v_0 r^2 / 6kT) \exp(-2r/r_0) \exp(-3/(4\pi r^3 N(E_f)kT)). \quad (6)$$

The combined factors within the exponential terms (i.e.  $(2r/r_0) + (3/(4\pi r^3 N(E_f)kT))$ ) are then differentiated with respect to  $r$ , to find the value at which the hopping probability is maximised:

$$r_{\text{max}} = (9r_0^3 / (8\pi N(E_f)kT))^{1/4}. \quad (7)$$

Substituting this value into Eq. (6), and *ignoring* the dependence of the pre-exponential factor upon  $T$  and  $r_{\text{max}}$ , one obtains:

$$\mu_{\text{hop}} = C \exp(-B/T^{1/4}). \quad (8)$$

The initial model outlined above was later *slightly* modified [1] by replacing the full sphere radius with an average (*un-weighted*) hopping distance within it, and thus defined as:

$$r_{\text{av}} = \int_0^r R^3 dR / \int_0^r R^2 dR = 3r/4, \quad (9)$$

in which case  $B = B_0(1/(r_0^3 kN(E_f))^{1/4})$ , with  $B_0 = 2(3/2\pi)^{1/4} = 1.66$ .

The model was attractive not only in (quite correctly, at a *qualitative* level) offering an explanation

of the observed deviations from Arrhenius behaviour at low temperatures, *but also in providing an attractively simple procedure for estimating  $N(E_f)$* . However, when this was attempted, very questionable values were often obtained (see below).

The error is that the model uses the parameter  $r$  both as the *distance hopped* and the radius of the sphere *within which hopping occurs* (or, in the revised version, 75% of this). This is equivalent to placing all sites within the sphere at its surface, as in Fig. 3c. The modification introduced in Eq. (9) does not resolve this problem, since the averaging still omits the exponentially decreasing probability of hopping as the inter-site separation increases. Including the factor  $\exp(-2r/r_0)$  in both the numerator and denominator of Eq. (9), and extending the upper limitation of the integration to infinity, yields an *average* hopping distance  $r_{\text{av}} = (r_0/2)(\Gamma(4)/\Gamma(3)) = 1.5r_0$ , i.e. 0.6 simulation units in the present case. Thus, there is no longer any dependence upon  $r$ , except at very small values (where  $r_{\text{av}}$  is even smaller) and therefore no prediction of variable range hopping!

It might seem tempting to modify this model by considering the *incremental* sites introduced when the sphere radius is increased slightly (i.e. replacing  $4\pi r^3/3$  by  $4\pi r^2 \Delta r$ ). However, this would not only yield a different ( $T^{-1/3}$ ) temperature dependence, but also any predicted value of  $N(E_f)$  would obviously depend upon the assumed value of  $\Delta r$ .

Finally, in this Section, we note that the term "variable range hopping" can give the impression that the increased hopping distance, *in its own right*, is the primary factor generating the non-Arrhenius behaviour. As shown below, the increase in hopping distance is less than a factor of 2 over the range 80 to 6K, for both the Mott model (Eq. 7) and our own calculations. Thus, it makes a relatively small *direct* contribution to the mobility, whereas the reduced activation energy accompanying it is by far the dominant factor.

## 5. Low-temperature "variable range" hopping – The computer simulation

As well as allowing the exploration of various aspects of carrier thermalisation, the Monte-Carlo procedure permits the study of the temperature dependence of mobility values, following the attainment of the eventual steady state.

As shown above, the various definitions of  $\mu$  and  $eD/kT$  yield values that all converge at sufficiently long times. Thus, to avoid noise limitations, and other possible distortions at finite fields, as mentioned above, the mobilities derived in this Section (temperature range 6 - 100K) were all obtained from diffusion (using Eq. 3a) data, obtained at zero applied field. Also (for safety in respect of the potential problems outlined in Section 2.1) transitions were allowed to 16 nearest neighbours. In practice, this yielded no detectable differences in the mobility or diffusion data, relative to the 8 neighbour

cases, except at the very lowest temperatures (where small increases in these parameters could be detected).

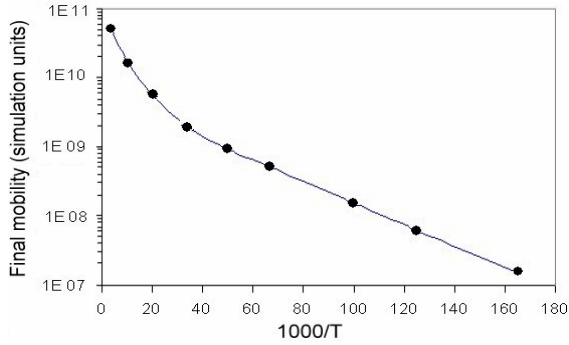


Fig. 8. Temperature dependence of the mobility after the completion of equilibration.

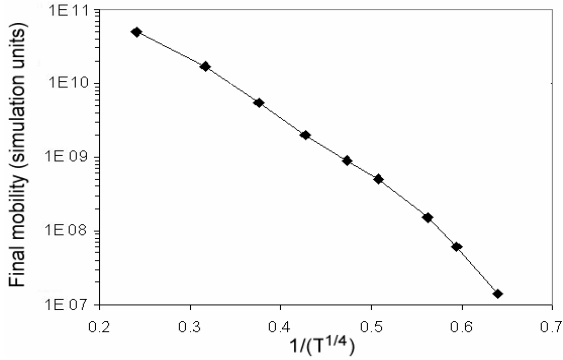


Fig. 9.  $1/T^{1/4}$  dependence of the mobility after the completion of equilibration.

Fig. 8 shows the temperature dependence of the final mobility, in an Arrhenius plot, and Fig. 9 shows the corresponding " $T^{-1/4}$ " plot. The latter obviously does not yield a good linear dependence. As noted above, such a plot ignores the effects of the parameters  $T$  and  $r_{\max}$  on the pre-exponential factor in Eqs. 6 and 7. Since  $r_{\max}$  is expected to vary as  $T^{-1/4}$ , the pre-exponential factor should vary as  $T^{3/2}$ . However, using  $\mu T^{3/2}$  as the vertical scale reduces, but does not eliminate, the curvature. Also, this plotting format does not appear to have been employed in practice, and certainly not in any of the examples cited in [1]!

For closer inspection, we used a commercial package (Origin 6.1) to fit the experimental low  $T$  (6 - 100K) data to equations of the form:

$$\ln(\mu) = A + B. t^{1/n} \quad (10a)$$

$$\ln(\mu. T^{3/2}) = A + B. t^{1/n} \quad (10b)$$

Table 1 shows the results, in terms of  $n$  and the associated statistical parameters  $\chi^2$  and  $\delta^2$  (where  $\delta$  is the coefficient of determination). The best results, in terms of both parameters, are clearly obtained for the free parameter fit to Eq. 10b, and the next best are for the corresponding Eq. 10a case (albeit with a *significantly*

different value of  $n$ !) The forced fit to Eq. 10a, with  $n = 4$ , gives by far the poorest statistical agreement. Fig. 10 illustrates the qualities of the two fits, for the raw mobility (as opposed to the  $\mu. T^{3/2}$ ) data.

Table 1. Free and forced (in terms of  $n$ ) fits of the mobility data to Eqs. 10a and 10b.

Fitting parameters	Free $\mu$	Forced $\mu$	Free $\mu^* T^{3/2}$	Forced $\mu^* T^{3/2}$
$n$	1.98	4	3.34	4
$\chi^2$	0.0268	0.0961	0.0353	0.0457
$\delta^2$	0.9966	0.9852	0.9982	0.9964

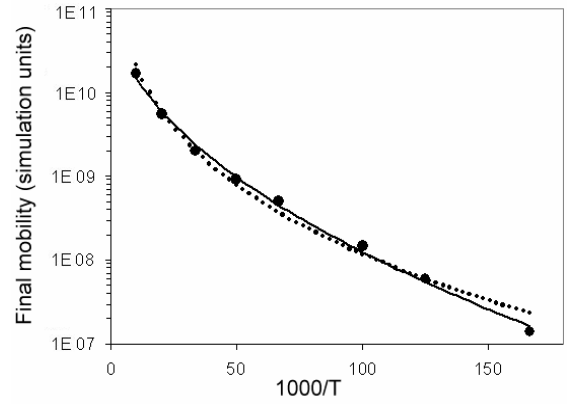


Fig. 10. A comparison of  $T^{-1/n}$  fits to the mobility data, using parameters  $n = 1.98$  (solid line) and  $n = 4$  (dotted line).

### 5.1. An alternative approach to the analysis of low temperature "variable range" hopping

If nothing else, Table 1 and Fig. 10 illustrate the extreme sensitivity of the application of a " $T^{-1/n}$ " model to the analysis of low-temperature hopping data (and thus of any parameters such as  $N(E_f)$  derived from it). Therefore, we now propose an alternative approach to such analysis, and evaluate its results in respect of our simulation data, in terms of its ability to calculate the controlling hopping distance, and thereby  $N(E_f)$ .

As suggested above and demonstrated below, the primary factor controlling the low temperature behaviour is the progressive reduction in the activation energy ( $E_{\text{act}}$ ) with falling temperature. Thus, its value can be determined from the local gradient at any given  $T$ , and then inserted into a conventional equation of the form:

$$\mu(T) = (e v_0 r^2 / 6kT) \exp(-2r/r_0) \exp(-E_{\text{act}}/kT). \quad (11)$$

By simple iteration (and taking proper account of its effect upon the  $(e v_0 r^2 / 6kT)$  and  $\exp(-2r/r_0)$  terms), a value of  $r = r_c$  can be selected to give agreement with the measured mobility, without any presumption of the

temperature dependence of  $r_c$ . Values of  $\nu_0$  and  $r_0$  are obviously required, and are known for the simulation model. However, they would unavoidably still need to be estimated in the case of experimental studies (see below).

The volume of a sphere of radius  $r_c$  is simply  $V_c = (4/3)\pi r_c^3$ , and can be assumed to contain, on average, one dominant site within the identified activation energy range of the occupied one (i.e. ignoring all other sites of inaccessibly higher energy or inaccessibly greater distance). Thus,

$$N(E_{\text{act}}) \sim 1/(V_c \cdot E_{\text{act}}) \quad (12)$$

The procedure obviously contains its own simplifications, *but requires no assumption of the functional form of the temperature dependence of the mobility pre-factors* (as in Eqs. 10a and 10b). Moreover, in principle, it does not appear to require an energy-independent  $N(E)$  over the temperature range investigated (n.b.  $kT$  covers the range 0.5 to 8.6 meV for the data in Figs. 8 to 10).

## 5.2. Application of the above approach to the simulation data

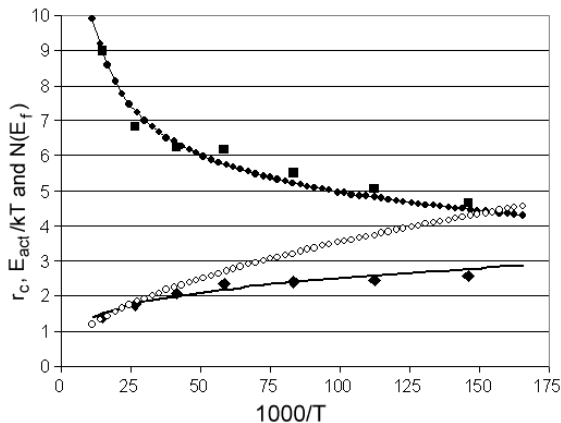


Fig. 11. Use of the model in Section 5.1 to give:  $r_c$  (solid line),  $N(E_f)$  (filled circles) and  $E_{\text{act}}/kT$  (open circles). The larger filled points were calculated directly from the simulation data, while the others were obtained using the solid line data in Fig. 10.

Fig. 11 summarises the results obtained by applying the procedure outlined in Section 5.1 to the present simulation data. We note that:

- (i) The calculated values of  $N(E_f)$  are within a factor of two of the actual value (an average site density of one simulation unit, spread uniformly over a 0.2 eV energy range gives  $N(E_f) = 5$  simulation units). Indeed, they are within 25% over most of the low temperature region.
- (ii) As suggested above, the hopping distance  $r_c$  only increases by a factor of  $\sim 2$  over the whole temperature range.

(iii) For *this*  $N(E)$ , and despite the increase in  $r_c$ , the activation energy does not fall significantly at low temperatures. In relative terms, it increases from  $\sim kT$  at the highest temperatures to  $\sim 5kT$  at the lowest ones. Thus, contrary to the Mott concept, carriers seem obliged to choose higher energy sites, due to the constraints imposed by the random spatial locations of the lowest energy ones.

Despite the above discrepancies, we have examined how the Mott model would fare, in computing  $N(E_f)$  when applied to the present data. Ignoring the clear curvature, a linear fit to the data in Fig. 9 was performed. It yielded  $B = 21 \pm 1$ , giving  $N(E_f) = 7.0 \pm 1.3$ . However, the more justifiable fit using  $\mu \cdot T^{3/2}$  (as in Eq. 10b) yielded  $B = 34 \pm 1$ , giving  $N(E_f) = 1.0 \pm 0.1$ .

It might also appear that, given the uncertainty in the assumed value of  $r_0^3$  in any *experimental* study, the above discrepancies could well be regarded as relatively minor (an error of only 2.15 in  $r_0$  produces a factor of 10 change in  $N(E_f)$ ).

$T^{1/4}$  plots for a considerable range of materials are presented in [1]. Although most do not include a calculation of  $N(E_f)$ , we have performed these, taking  $r_0 = 10^{-7}$  cm (the most commonly assumed value in [1]). This gives values of  $\sim 10^{18} - 10^{24}$  cm $^{-3}$ eV $^{-1}$ , and figures as high as  $10^{28}$  cm $^{-3}$ eV $^{-1}$  have been obtained elsewhere (e.g. [7]). Here, we note the statement ([1], p. 359) that: "*a density of states as high as  $10^{21}$  cm $^{-3}$ eV $^{-1}$  would almost certainly lead to delocalization and a metallic-like conductivity*" (i.e.  $r_0$  would approach or exceed the mean site separation close to  $E_f$ ). This was the case for about 50% of the data sets that we examined!

Finally, we note that temperature dependence is predicted to differ when the localised states above  $E_f$  are not distributed isotropically in energy, as assumed here and in the Mott model. Indeed, various analyses have been made of such cases (see e.g. [1] for examples and related comments).

We consider that most, if not all, of the problems outlined above are likely to remain in such cases. However, we repeat that the approach in Section 5.1 does not specifically require such an energy-independent  $N(E)$ . Initial studies suggest that the procedure can indeed cope with other forms of  $N(E)$ , albeit with a reduced precision so far, due to the need for even longer simulation runs to ensure that equilibration is fully achieved.

## 6. Conclusions

Monte Carlo simulation has been employed to examine hopping conduction in disordered solids.

Initial equilibration was shown to be a complex process, leading to a violation of the Einstein relationship between the mobility and diffusion coefficient, and reasons for this were advanced.

Attention was then directed to the "variable range hopping" regime, using the simulation data after completion of equilibration. The problems with the

Mott  $T^{-1/4}$  model were reviewed. A new alternative procedure was then advanced, and shown to give good agreement with the data.

Finally, the viability of using real experimental data to derive parameters such as the density of localised states close to the Fermi level was discussed. It was concluded that current procedures are questionable, at best. Further studies will establish whether our new procedure remains valid in the case of an energetically varying  $N(E)$  close to the Fermi level, and/or when the correct finite-temperature Fermi-Dirac statistics are used to describe the distribution of *empty* states close to  $E_f$ .

### Acknowledgements

The author thanks Professor Charles Main for a long (almost 40 years!) friendship and many productive discussions regarding this study.

He also acknowledges the stimulation provided by the late Professor Vladimir Arkhipov, via his incisive papers concerning low temperature hopping and other topics, and for suggested avenues for the present study. Vladimir will be sadly missed by many in our scientific community!

### References

- [1] N. F. Mott, E. A. Davis, *Electronic Processes in Non-Crystalline Materials*, Clarendon Press, Oxford (1979).
- [2] A. Miller, E. Abrahams, *Phys. Rev.* **120**, 745 (1960).
- [3] J. M. Marshall, V. Arkhipov, *J. Optoelectron. Adv. Mater.* **7**, 43 (2005).
- [4] J. M. Marshall, *Phil. Mag. Lett.* **80**, 691 (2000).
- [5] N. F. Mott, *J. Non-Cryst. Solids* **1**, 1 (1968).
- [6] N. F. Mott, *Phil. Mag.* **19**, 835 (1969).
- [7] D. K. Paul, S. S. Mitra, *Phys. Rev. Lett.* **31**, 1000 (1973).

---

\*Corresponding author: JoeMarshall@kiley9.freemove.co.uk